Loss of function of the RNA export factor, *Nxt1*, in *Drosophila* causes muscle degeneration and reduced expression of genes with long introns.

Kevin van der Graaf and Helen White-Cooper*

School of Biosciences, Cardiff University, Museum Avenue, Cardiff, United Kingdom

* Corresponding author, E-mail: white-cooperh@cf.ac.uk

Short title "RNA export factor Nxt1 ensures muscle integrity and maintenance"

Abstract

The RNA export pathway is essential for export-competent mRNAs to pass from the nucleus into the cytoplasm, and thus is essential for protein production and normal function of cells. *Drosophila* with partial loss of function of *Nxt1*, a core factor in the pathway, show reduced viability and male and female sterility. The male sterility has previously been shown to be caused by defects in testis-specific gene expression, particularly of genes without introns. Here we describe a specific defect in growth and maintenance of the larval muscles, leading to muscle degeneration in *Nxt1* mutants. RNAseq revealed reduced expression of mRNAs of many genes in *Nxt1* mutant muscles. Despite this, the degeneration was rescued by increased expression of a single gene, the costamere component *tn (abba),* in muscles. Genes under-expressed in the mutant typically have long introns, and most normally encode circular RNAs in addition to mRNAs. This is the first report of a specific role for the RNA export pathway gene *Nxt1* in muscle integrity. Our data on *Nxt1* links the mRNA export pathway to a global role in mRNA expression of genes that also produce circular RNAs, *in vivo.*

Author summary

In eukaryotic cells the DNA encoding instructions for protein synthesis is located in the nucleus, it is transcribed to generate pre-mRNA, which is processed at both ends and spliced to remove internal spacer regions (introns) to generate mRNA. This mRNA is then transported by the mRNA export pathway via nuclear pores to the cytoplasm for protein synthesis. We have previously shown that reduction in activity of a specific protein in the mRNA export pathway, Nxt1, has an additional role in testis-specific transcription. Here we describe a further role for this protein specifically in gene expression, particularly of genes with long introns, and in muscle maintenance. *Drosophila* larvae

with reduced Nxt1 activity have normal muscle pattern when they are small, but show muscular atrophy and degeneration as they grow, resulting in significant defects in their movement speed. We discovered that expression of many genes is reduced in the mutant larvae, but that restoring the expression of just one of these, *abba*, the *Drosophila* homologue of *Trim32* (a human gene involved in muscular dystrophy) is capable of preventing the muscle degeneration.

Introduction

The formation, growth and maintenance of the musculature is critical for normal animal function, and defects in these processes can lead to impaired mobility, shorter lifespan or early lethality. The somatic muscular tissue of *Drosophila* is generated via a highly regulated developmental programme in embryogenesis, such that the first instar larva contains a stereotyped pattern of muscles [1]. The abdominal A2-A7 segments each contain 30 muscles on each side of the animal, each with defined size, shape, position and attachment sites. Each muscle is a single multinucleated cell, derived from fusion of muscle founder cells with fusion competent myoblasts (reviewed in [2]). Very severe defects in embryonic myogenesis result in a failure of the embryo to hatch; less severe defects in the development of the muscle pattern or in muscle function can result in animals with impaired mobility. During larval stages no new cells are added, but the muscles grow extensively by addition of new myofibrils, particularly during the final larval instar (reviewed in [3]).

Normal muscle function is essential during pupariation, and defects in larval muscles can lead to lethality at this stage. About 12 hours before pupariation a pulse of ecdysone triggers the larvae to stop feeding, and move out of the food. About 6-10 hours later they stop moving, contract longitudinally, evert their spiracles and become a white pre-pupa. Three hours later the prepupa contracts from the anterior partially withdrawing the anterior tracheal lining [4]. At this stage an air bubble forms in the abdominal cavity. The bubble gradually increases in size and the abdominal tissue is forced against the body wall. One hour later, the prepupa becomes separated from the puparium due to the secretion of the prepupal cuticle. The air bubble migrates to the anterior by abdominal muscular contractions, creating space inside the puparium to evert the head, which up to this point has been developing internally. Contraction of the tip of the abdomen permits the elimination of the air bubble via the spiracles [4]. Orchestration of these events requires pristine muscle function

Regulation of gene expression is important for the normal development and functioning of organelles, cells, tissues and the whole organism. Regulation of mRNA expression depends on transcriptional regulatory processes, such as transcription factor and repressor binding that influence the ability of RNA polymerase to bind to the promoter site and carry out transcription. Post-

transcriptional regulation of RNA adds additional layers of potential control, both in the nucleus and after mRNA export to the cytoplasm. Within the nucleus, critical processing and control points include (alternative) splicing of exons and association of the RNA with mRNA nuclear export factors. The passage of the mRNA transcripts to the cytoplasm requires the export factors associated with the transcript to be recognized by receptors in the interior of the pores (reviewed in [5]). The association of nascent RNA with export factors occurs co-transcriptionally and involves first the binding of hnRNPs to the transcript, then recruitment of the THO export complex, and finally recruitment of a heterodimer of Nxf1/Nxt1. The THO complex interacts with UAP56 and REF to form transcription-export complex (TREX) [6]. During the recruitment of Nxf1/Nxt1, export factors such as UAP56 and THO complex are displaced from the RNA. Splicing of pre-mRNAs not only results in removal of the intron sequence from the transcript, but also results in the deposition of a protein complex, the Exon Junction Complex (EJC) 5' of the splice junction. The EJC has many regulatory roles, including acting to help recruit the RNA export components, and thus facilitates nuclear export of correctly processed mRNAs (reviewed in [7]).

Circular RNAs (circRNAs) are a recently discovered class of RNAs generated by splicosome-dependent back splicing of segments of primary transcripts (reviewed in [8, 9]). The 3' end of an exon splices to the 5' end of the same exon, or to a further upstream splice acceptor site in some cases. The production of circRNA depends on alternative transcript processing; typically the exon that is circularized is not subject to conventional alternative splicing, but is flanked by relatively long introns [10]. Modulation of transcription rate and splicing rate both affect the relative efficiency of forward and back splicing events, and thus can alter the expression level or ratio of the alternative products [11, 12]. CircRNAs are relatively stable, and, while typically of relatively low abundance, they can accumulate to levels equal to or even exceeding that of the mRNA(s) derived from the same gene. Analysis of total RNA sequencing data has revealed at least 2500 circRNAs expressed in *Drosophila* [13]. CircRNAs are particularly abundant in neural tissue, but all analysed tissues express some circRNAs [13]. CircRNAs have been shown to have a variety of roles *in vivo*, including acting as miRNA sponges, protein sponges, protein scaffolders and being translated (reviewed in [8, 9]).

Human muscular dystrophies are a group of inherited genetic conditions that cause muscles to weaken, leading to an increasing level of disability. Muscular dystrophy is typically caused by mutations in genes involved in muscle structure. Duchenne muscular dystrophy, one of the most common and severe, is caused by mutations in *dystrophin* [14], that encodes a component of the costamere, a complex that connects the muscle fibre cytoskeleton to the extracellular matrix [15]. Similarly, limb girdle muscular dystrophy 2H is caused by defects in *Trim32*, another costamere subunit [16]. Myotonic dystrophy in contrast is typically caused by defects in RNA metabolism

(Reviewed in [17, 18]). In DM1 myotonic dystrophy, a trinucleotide repeat in the 3' UTR of the *DMPK* gene results in sequestration of the splicing regulator MBNL1, and this in turn causes defects in muscle gene expression, particularly alteration of splicing patterns. Similarly in DM2 myotonic dystrophy a CCTG repeat in the intron of ZNF9 results in the generation of a pathogenic RNA that also sequesters MBNL1. Interestingly both MBNL1 and *muscleblind* (*mbl*), the *Drosophila* orthologue of MBNL1, produce abundant circular RNAs [11]. Moreover, Mbl protein is implicated in regulation of production of its own circRNA [11], although the MBNL1 circRNA has not yet been implicated in myotonic dystrophy [19].

We have previously described a role for Nxt1 in regulation of transcription in *Drosophila* testes, indicating that the level of this gene product is critical for processes beyond its known role in mRNA nuclear export [20]. Here we describe a specific role for Nxt1 in the maintenance of larval muscles. Specifically, *Nxt1* partial loss of function animals show muscle degeneration during the extensive growth associated with the final larval instar stage. We rescued the muscle degeneration, but not the pupal lethality, by expression of the Drosophila homologue of *Trim32*, *tn (abba)*, in muscles. We show that normal expression of many genes, particularly those with long introns that are sources of circRNAs, requires Nxt1. Together our data indicate an unexpected role for Nxt1 in post-transcriptional regulation of many genes, and show that this ubiquitously required RNA export protein is essential for muscle maintenance.

Results

Nxt1 pupae have a distinctive curved shape, uneverted spiracles and fail head eversion

We have previously described that $Nxt1^{z2\text{-}0488}$ / $Nxt1^{DG05102}$ transheterozygotes are male and female sterile, but also have significantly reduced viability [20]. Many $Nxt1^{z2\text{-}0488}$ / $Nxt1^{DG05102}$ transheterozygote pupae had a curved shape and uneverted spiracles (Figure 1A). To quantify this morphological defect we measured the axial ratios from the pupa by measuring the length (excluding the posterior and anterior spiracles) and width. This confirmed that the mutant pupae were significantly longer and thinner than wild type. Scanning electron microscopy (SEM) revealed that the surface structure of the pupal case was similar between mutant and wild type (Figure 1C-E), however, in Nxt1 trans-heterozygotes, 50% (N=36) had uneverted anterior spiracles (Figure 1E'').

We have also previously reported that the $Nxt1^{z2\text{-}0488}$ / $Nxt1^{DG05102}$ transheterozygote pupae show failure in head eversion [20]. Air bubble formation and migration is implicated in head eversion and

therefore the viability of the pupa. To analyse this process we filmed w^{1118} and $Nxt1^{z2\text{-}0488}$ / $Nxt1^{DG05102}$ trans-heterozygote pre-pupae and for 15 hours to observe the air bubble; a typical series is shown. (Figure 2) In wild type controls head eversion occurs at around 12 hours into the pupa phase (Figure 2M). Before the head eversion occurred, there was a dramatic period of muscular contractions, as the posterior of the larva wriggled then contracted towards the anterior. At the same time as head eversion the whole larva body wriggled back within the pupal case to reach the posterior end. The air bubble formed normally in the mutants, and was faintly visible from 0h APF, growing in size over the next few hours (Figure 2A), however air bubble migration stalled by 8h APF (Figure 2I) and it remained in the middle of the pupa until 11h APF (Figure 2J-M) before disappearing and leaving an empty space at the posterior of the pupa body (Figure 2N-P). No head eversion was seen in this mutant pupa (Figure 2M).

Crosses of $Nxt1^{DG05102}$/*CyO, Act-GFP* to $Nxt1^{Z2\text{-}0488}$/ *CyO, Act-GFP* did not reveal the expected Mendelian ratios of 1:2 (Nxt1 trans-heterozygotes: *CyO, Act-GFP;* note *CyO, Act-GFP* homozygotes are lethal). Instead, the observed ratio was 1:10. We assessed the progression of pupal development at four time points (24h, 48h, 72h and 96h pupa), and the number of viable adults. Only about 20% (N=182) of the Nxt1 trans-heterozygote pupae survived through to adulthood, compared to 90% (N= 287) viability for control w^{1118} pupae (Figure S1). The $Nxt1^{DG05102}$/+ showed a slight reduction to pupa viability (60% (N= 211); Figure S1). Head eversion occurs roughly 12 hours in the pupa stage, however, pupa metamorphosis continues to develop (such as body, bristles and wings) in Nxt1 trans-heterozygotes where most pupa do not have head eversion. The consequence of no head eversion was seen between 48-96 hours in the metamorphosis where the development stopped abruptly, and the pupa blackened.

Ecdysone-responsive gene expression is not affected in *Nxt1* mutants

The air bubble phenotype suggests that there are defects in the function of the larval/pupal abdominal muscles, or in the developmental regulation of their function at this stage. Ecdysone coordinates tissue-specific morphogenetic changes by several pulses throughout the *Drosophila* development (reviewed in [29]). A high concentration pulse is observed immediately preceding the larva-pupa transition, and this pulse is essential to trigger the muscular contractions on pupariation and in the pre-pupa. To understand if a transcriptional defect downstream of ecdysone signalling is responsible for the phenotype, in a manner analogous to the role for Nxt1 in regulation of tMAC-dependent testis-specific transcripts, we performed RNA sequencing of pooled whole larvae before (wandering larvae), during (stationary larvae), and after (white prepupae) the pulse of ecdysone.

We extracted the expression data for known ecdysone-responsive genes [30] looking for (1) differential expression between mutant and control, (2) minimum of 2-fold up or down regulated and (3) a minimum FPKM value of 10 in at least one condition. Out of 87 ecdysone-responsive genes only four were mildly mis-regulated, others were unchanged (Supplementary Table 1). None of these

genes have an air bubble phenotype when down regulated [31, 32], therefore, it is unlikely that failure of expression of ecdysone-responsive genes is responsible for the air bubble phenotype in Nxt1 trans-heterozygotes.

Muscle degeneration occurs in *Nxt1* mutant larvae

To determine whether the defects seen in pupal and pre-pupal stages in *Nxt1* mutants are due to muscular defects we characterized the structure and function of muscles in the larval stages. A larval movement assay was used to track 1st, 2nd, and 3rd instar larvae to compare their speed between w^{1118} and Nxt1 trans-heterozygotes. Larvae were tracked on an agar plate with a control odor on each side (Figure 3A and B). These experiments showed that there was no significant difference in the average speed of mutant larvae compared to wild type at either 1st or 2nd instar stage. Normally there is a dramatic increase in migration speed after the last larval molt; wild type 3rd instar larvae travel up to 5x faster than 2nd instars (Figure 3F). In contrast, Nxt1 trans-heterozygous 3rd instar larvae were no faster than 2nd instar larvae (Figure 3G), despite being much larger. Thus, mutant 3rd instars were significantly slower than control animals (Figure 3C-G).

To investigate the muscle structure in the mutant animals we stained of 3rd instar larval body wall muscles with phalloidin which labels F-actin. In *Drosophila* larvae, each of the abdominal hemisegments A2-A7 has a stereotypical pattern of 30 different muscles [1]. This pattern was clearly observed in the wild type (Figure 4A and C), however, $Nxt1^{z2\text{-}0488}$ / $Nxt1^{DG05102}$ trans-heterozygotes showed clear signs of muscle degeneration (Figure 4B, D and E). Defects seen were variable, and included thinner muscles, fiber splits and torn muscles (Figure 4F-K). We counted the number and nature of defective muscles in 8 hemisegments of 6 control and 6 mutant third instar larvae and categorized the nature of the defects. Defects seen in the mutants were variable and included thinner muscles (15%), loss of sarcomeric structure (22%), degenerating muscles (77%), torn muscles (8%); all control animals had no defects.

In addition to the gross morphological defects, $Nxt1^{z2\text{-}0488}$ / $Nxt1^{DG05102}$ trans-heterozygote mutant animals also sometimes had defects in internal muscle structure. Normal muscle sarcomere structure consists of thick and thin filaments, and phalloidin staining of actin reveals this structure by labelling the thin filaments in the sarcomere (Supplementary Figure 2A). For Nxt1 trans-heterozygotes, the sarcomere structure was compromised in 22% of the muscles examined. These muscles showed more uniform phalloidin staining indicating weak or absent differentiation of thin vs thick filaments (Supplementary Figure 2C). This muscle degeneration and sarcomere structure defect phenotype was not fully penetrant, and some Nxt1 trans-heterozygotes had more normal sarcomere structure and less obvious muscle degeneration. This is consistent with the finding that about 20% of the mutant third instar larvae are able to develop to adulthood (Supplementary Figure 2B). We analysed muscles from first (N=8) and second (N=10) instars with phalloidin staining. This

revealed that earlier stage larvae have a normal musculature, and thus that the defects are due to degeneration rather than a developmental defect.

To confirm that the muscle phenotype observed was due to defects in Nxt1 rather than being a non-specific effect we used Mef2-Gal4 to drive UAS-RNAi and UAS-dicer expression specifically in muscles. Both RNAi lines 103146 (chromosome 2) and 52631 (chromosome 3) had previously been shown to effectively knock down *Nxt1* and phenocopy the mutant phenotype in spermatocytes [20]. Phalloidin staining of these 2nd instar larvae showed extensive muscle degeneration (Supplementary Figure 3). When the temperature was 25^{o}C for embryonic development, with a shift to 29^{o}C after hatching line 52631 still induced early 2nd instar lethality. Line 103146 gave a phenotype very similar to the *Nxt1*$^{z2\text{-}0488}$ / *Nxt1* ^{DG05102} trans-heterozygote hypomorphic condition. This indicates that knock down of Nxt1 specifically in muscles is able to phenocopy the Nxt1 mutant situation, and shows that the degeneration is due to reduction in Nxt1 activity in muscles.

We expressed GFP-Nxt1 via the UAS-gal4 system both exclusively in muscles and ubiquitously with mef2gal4>UAS-GFP-*Nxt1* and armgal4>UAS-GFP-*Nxt1* in Nxt1 trans-heterozygotes. mef2gal4>UAS-*Nxt1* was able to partially rescue muscle integrity in Nxt1 trans-heterozygotes (~13-26% with two 47% outliers (N= 10)) and partially rescue the pupa lethality (~40% (N= 186)). On average, the axial ratios were similar to wild type, albeit more variable. Finally, mobility was increased compared to Nxt1 trans-heterozygotes, but was still significantly reduced compared to wild type (Student's t-test * $p<0.05$). Armgal4>UAS-GFP-*Nxt1* in Nxt1 trans-heterozygotes also showed improved, but not fully rescued muscle integrity (~3-33% damage with one 73% outlier (N= 9), increased the pupa viability (~75% (N= 163)) and increased larval mobility. The axial ratios were similar to wild type.

Growth of muscles causes muscle degeneration

During the last instar phase, larvae will grow substantially compared to earlier instars. Larvae removed from the food 70 hours after egg laying do not grow, but still crawl until the normal time for pupation (~112 hours AEL) and may survive through to adulthood, generating very small flies [33]. Larvae at 70 hours AEL are late 2nd, or early 3rd instars.

To test whether growth or use (movement) is implicated in the muscle degeneration in *Nxt1* mutants we fed ~60 larvae for 70-73 hours then removed them from the food. 14-25% of the larvae (removed from food at 70-73 hr) were able to pupate although less than 5% of those pupae were able to emerge as adults. We simultaneously examined ~60 of the Nxt1 trans-heterozygote larvae that were starved from 70-hour AEL and found, similar to w^{1118}, that only a few larvae pupated, and none emerged as adults. The pupae that formed had everted spiracles (Figure 5A) and resembled the wild type controls. Interestingly, the larvae that failed to pupate were able to survive for several additional days as larvae before dying. Nxt1 trans-heterozygote larvae were dissected four days after they were removed from the food, and were stained with phalloidin. For all larvae (n=10), no

muscle degeneration was observed (Figure 5B). These larvae had been moving normally and thus using their body wall muscles for the four days of starvation. The lack of abnormalities in these animals indicates that it is the muscle growth rather than use that is critical for degeneration in *Nxt1* mutants.

Increased expression of *abba* rescues the muscle degeneration, but not semi-lethality

The known role of Nxt1 in RNA export and transcriptional control suggested that the muscle phenotype could be due to defects in gene expression. To examine this, the RNA expression of 13 known muscle-specific or muscle-enriched genes was analysed in the whole larva RNA-seq data (Supplementary Table 2). Nine genes were more than 1.5-fold up regulated, with only one down regulated in the mutant larvae. *abba* (also known as *thin* (*tn*)), the only gene down regulated in this list, is an essential TRIM/RBCC protein that maintains integrity of sarcomeric cytoarchitecture [22]. Loss of function mutations in *abba* cause lethality, with the larvae and pupae being long and thin and having muscle degeneration [34]. *abba* is a large gene with several long introns and has a RING finger, B-Box & CC-domain and several NHL repeats (Figure 6A). qRT-PCR of samples made from 30 mutant larvae compared to 30 wild type larvae confirmed the reduction in *abba* expression. 10 individual stationary larvae were also compared to a pool of 10 wild type stationary larvae. This revealed the level of *abba* to be highly variable between individuals; *abba* mRNA was significantly down regulated in 9 out of 10 larvae (Figure 6B). To determine whether reduction in the expression of *abba* was implicated in the mutant phenotype we used a UAS-*abba*$^{\text{full length (fl)}}$ cDNA construct (kindly gifted by Hanh T. Nguyen; hereafter referred to as UAS-*abba*) and expressed it under the muscle specific driver mef2-gal4 in the *Nxt1* trans-heterozygote background. Staining of the muscles of these larvae with phalloidin, showed that for 12 out of 16 the muscle degeneration was fully rescued, and for the other four animals there was partial rescue (Figure 6C). qRT-PCR of 10 individual stationary larvae, compared to a mix of 10 wild type stationary larvae, again showed high variability between individuals, but 8 out of 10 had *abba* expression equal to or exceeding that seen in wild type (Figure 6D).

abba has at least six isoforms with 13 exons in its longest transcript and contains introns up to 4 kb in length (FlyBase). We compared nascent (primers in introns) versus spliced (primers in adjacent exons) transcript expression by Q-RT-PCR to determine whether transcription of the gene was altered in mutants, or whether the reduction in mRNA detected was due to a post-transcriptional defect. Four different regions were selected that would target as many isoforms as possible (Figure 7A). Interestingly, all regions throughout *abba* had similar expression of nascent transcript in mutant compared to control animals, but the levels of spliced transcript were reduced in mutants compared to control (Figure 7B). Thus, loss of Nxt1 does not impact on *abba* transcription, but Nxt1 is important for efficient production of the processed mRNA from the primary transcript.

Genes with long introns that also produce circRNAs are sensitive to the loss of Nxt1

The genetic rescue experiments indicate that the muscle defect in Nxt1 mutant larvae is primarily due to the reduction in *abba* expression. We examined the ability of these animals to survive to adulthood and found that the lethality was not rescued (22%; N=187) and thus must be caused by a different mechanism. Nxt1 is important for mRNA export, is recruited indirectly by EJC to spliced transcripts [35], and mutations in the EJC can cause reduced accumulation of transcripts with long introns [36]. In contrast, in Nxt1 trans-heterozygote testis, transcripts from short and intron-less genes were dramatically reduced, and inclusion of at least one intron increased transcript production [20].

To determine which other genes were differentially expressed in *Nxt1* muscles, compared to wild type and how these could be regulated by an RNA processing component, we performed new RNA sequencing from third instar larval carcasses. Each genotype (w^{1118} and Nxt1 trans-heterozygotes) was performed in triplicates. The numbers of significantly up- and down-regulated genes are shown in Table 1. We initially analysed the total intron length, number of introns and smallest/largest intron. This revealed that, in direct contrast to the situation in testes, down-regulated genes had more introns and a higher total intron length than non-differentially expressed genes, while up-regulated genes had fewer introns and a lower total intron length than the genes that were not differentially expressed genes (Mann-Whitney test p-value <0.05, except for 16-fold up regulated (p value of 0.16)); (Table 1 and Figure 8). We extended the analysis by also looking at the gene length and shortest/longest transcripts (Table 2). Again, a clear trend showed that down-regulated genes had longer median mRNA length and up-regulated genes had shorter median mRNA length when compared to non-differentially expressed genes (Mann-Whitney p<0.05; Table 2). Finally, the genes down regulated in *Nxt1* mutants produced more distinct mRNA isoforms than those up regulated or not differentially expressed (Table 2). qRT-PCR for 12 genes with high total intron length confirmed the down-regulation seen in the RNA sequencing data (Figure 9). *abba*, with a total intron length of approximately 41,000bp, was down regulated as expected and *Nxt1*, with a total intron length of 184bp, was only mildly affected (Figure 9).

Long introns present a challenge to the splicosome, and indeed some long introns are spliced as several shorter fragments via recursive splicing [37]. 116 genes are known to be processed via recursive splicing, of these, expression of 112 was detected in our RNAseq sample. Only 11 of these were 8x or more down-regulated in the *Nxt1* mutants (34 were 4x or more down-regulated). We therefore concluded that Nxt1 is unlikely to be required for recursive splicing per se, and considered other aspects of genes with long introns.

Genes with long introns are sources of circular RNAs, with many circular RNA exons being flanked by long introns. We therefore compared the genes down-regulated in *Nxt1* muscles with lists of genes known to produce circRNA transcripts [13], and found a striking overlap. 466 of the 567 genes 4x or more down-regulated in *Nxt1* muscles had at least one read consistent with a circRNA. 199 of

these genes were in the higher confidence set associated with at least 10 circRNA reads. 57 of the 186 genes that were at least 8x down regulated in *Nxt1* muscles were also in the high confidence circRNA set. circRNAs are also predominantly produced from genes that are known to have neuronal functions and whose expression is higher in nervous system, even when the analysis is performed on tissues outside the nervous system [13]. Consistent with this, embryonic expression pattern enrichment analysis via FlyMine revealed that the genes down-regulated in *Nxt1* muscles are indeed significantly enriched for expression in nervous-system (such as ventral nerve cord (p=1.13e-8), embryonic brain (p=3.06e-6)). We conclude that Nxt1 is important not only for the export of mRNAs but also for the normal mRNA expression levels of mRNAs from genes with long introns, particularly those that produce circRNA products.

Discussion

Reduction in Nxt1 function causes muscle degeneration

Nxt1 is primarily known for its role in the RNA export pathway. Nxt1 binds to Nxf1, which interacts with the nuclear pore complex for exporting mRNA to the cytoplasm [38]. Reducing Nxt1 reduces the Nxt1-Nxf1 dimer and without Nxt1, Nxf1 interacts less effectively with the nuclear pore complex [39]. Since most mRNAs are exported via the Nxt1-Nxf1 route, it is expected that many transcripts will be affected, and indeed this is what is seen in tissue culture cells [38]. Consistent with this, homozygotes of the null *Nxt1* allele are embryonic lethal. The hypomorphic allele we have used retains sufficient Nxt1 activity, even when in trans to a null allele, to support mRNA export, and thus allows us to explore other functions of this protein. Intriguingly, the transheterozygotes are able to develop apparently normally to the third instar larval stage, and to undergo pupariation. Most lethality occurred at this transition, with obvious defects in air bubble migration and pupal shape. The phenotype is not fully penetrant, and some Nxt1 trans-heterozygote pupae had normal morphology; 20% of transheterozygote third instar pupae survived through to adulthood.

The defects in pupal morphology are caused by muscle degeneration during the third instar larval stage. Muscles of the second instar larvae had normal pattern, normal morphology and these animals had normal motility. This indicates that the establishment of the larval musculature, which occurs during embryonic development, is not affected by the reduction in Nxt1 in the hypomorphic allele.

Muscles are composed of tandem arrays of sarcomeres containing thick and thin filaments, arranged in myofibrils. When a muscle twitches, the filaments slide past each other in response to calcium release from the sarcoplasmic reticulum (SR) resulting in force generation. Our examination of the muscle integrity in transheterozygote larvae revealed a variety of defects including muscle atrophy (thinning) and loss of integrity (tearing and splitting). Frequently we saw loss of filamentous actin in the middle of the muscle while the ends had f-actin; very occasionally we saw balls of muscles associated with loss of attachment or catastrophic failure of muscle integrity and muscle severing.

Even when the muscle shape was unaffected we found a loss of normal internal architecture with disruption of the sarcomeric arrays. Often the muscle was present, but there was filamentous actin staining only towards the ends of the muscle and the central region lacked the sarcomeric structure. It is likely that the reduction in larval mobility, the axial ratio defect, the failure of spiracle eversion and the failure of air bubble movement are all a direct result of the degeneration of muscles in the mutant larvae. All these processes require efficient and coordinated muscle contractions, which are compromised by lack of Nxt1. The curved shape of many mutant pupae is likely to be due to the variability in extent of muscle degeneration, if an individual has more damage on one side, particularly of the longitudinal muscles, than the other there will be unequal contraction as the prepupa forms, and one side of the body will shorten more.

During the larval phase, the muscles undergo a ~50-fold increase in fibre size. This dramatic growth occurs without addition of new cells, as the nuclear number remains constant. Increased DNA content is achieved via endoreduplication, and increased volume is driven by cell growth associated with new myofibril and sarcomere assembly [3]. The majority of this growth occurs during the third instar larval stage, and depends on nutrient supply and sensing of this via the Insulin/Akt/Tor pathway [40]. Deficits in muscle growth, for example caused by reducing endoreduplication through over expression of cyclinE in muscle, have non-autonomous effects on the growth of the whole larva [40]. We did not detect any difference in the overall size of the third instar mutant larvae, indicating that the defects are not due to defects in nutrient supply or sensing. When Nxt1 hypomorphic larvae are starved from the late 2nd or early 3rd instar larval stage they remain alive and continue to move, but growth is blocked. This treatment was sufficient to rescue the muscle degeneration that typically occurs during the 3rd instar phase. This indicates that the primary cause of the degeneration is defective (re)-organisation during muscle growth, rather than damage caused by use of the muscles.

Muscle degeneration can be rescued by increasing *abba*

We were surprised that a hypomorphic allele of a pleiotropic factor such as Nxt1 had such a specific phenotype of muscle degeneration, and reasoned that, while it is likely to be important for the normal expression of many genes, reduction in just one or a few crucial genes could underpin the muscle defects. Our RNA-seq of whole larvae was a mixed sex population, and unfortunately the majority of genes differentially expressed between samples were those with testes-specific or testis-enriched expression. This is consistent with our previous findings that Nxt1 is critical for expression of genes regulated by tMAC in testes, but meant that the signal from relatively mild expression changes from somatic tissues was less apparent. Nevertheless one gene, *abba*, with a known role in muscles stood out as being mildly down-regulated, and qRT-PCR data confirmed that *abba* was indeed down regulated in 9 out of 10 stationary larvae (Figure 6B). The phenotype of *abba* mutants is strikingly similar to that we describe for *Nxt1* hypomorphs, particularly with thinner muscles, long thin pupae and defects in both spiracle eversion and air bubble migration [22, 34]. Abba is a TRIM/RBCC protein

involved in maintaining the integrity of sarcomeric cytoarchitecture [22, 34], and is the *Drosophila* homologue of human *Trim32*, defects in which cause limb girdle muscular dystrophy 2H [16]. Trim32 is localised to the costamere, which overlies the Z-disk and ensures attachment of the sarcomere to the overlying extracellular matrix via the dystrophin glycoprotein complex.

The reduction in abba expression in *Nxt1* mutants, probably in combination with reduction in other factors, would cause defects in costamere assembly or function. This would then lead to defects in maintenance of muscle integrity and progressive loss of muscle structure. The phenotypes of defective sarcomere structure, fraying and muscular atrophy are all consistent with reduction in *abba* (costamere) function. The growth of muscles involves the generation of new sarcomeric units, each requiring a new costamere and thus new Abba production and incorporation. The gradual decline in muscle integrity seen during growth may then be attributable to reduction in Abba protein levels meaning that the stability of newly formed sarcomeres is reduced. Indeed, in mouse the expression of Trim32 is upregulated in muscles that are remodelling [41]. Increasing expression of *abba* using a cDNA construct driven with the Gal4/UAS system is sufficient to rescue the muscle defects seen in *Nxt1* mutants, consistent with this model. Starvation from late second or early third instar larval stage is also sufficient to rescue the muscle defect. In this case there is no muscle growth, so no new sarcomeric units need to be added, the existing structures are maintained, and thus there is no muscle degeneration.

RNAi constructs to disrupt Nxt1 function in muscles caused degeneration, again without pattern defects, even in second instar larvae, indicating that the precise level of Nxt1 function is critical. Presumably the RNAi construct expression, driven in by the strong muscle-specific driver, Mef2-Gal4, from embryonic stages, reduces the level of active Nxt1 in muscles in embryos and early larval stages even beyond that which we see in the hypomorphic allele combination. In this situation there would be reduced Abba both during embryonic muscle formation and at the early growth stages, and this would impact on the muscle integrity even before the extensive third instar larval growth period. Importantly, this experiment confirms that the phenotype is caused by reduction in Nxt1 function rather than by a different gene or by a neomorphic effect of the point mutation in $Nxt1^{Z2\text{-}0488}$.

Nxt1 is particularly important for expression of transcripts from genes with long introns

abba is a long transcription unit that contains several long introns. Transcripts with many and large introns could be more vulnerable towards the loss of Nxt1, based on the finding that genes with long introns were sensitive to the loss of the EJC [42]. In direct contrast, in testes, genes without introns were particularly sensitive to loss of *Nxt1* [20]. RNA-seq data from larval carcasses, which is highly enriched for larval muscles, allowed us to specifically examine the role of Nxt1 in transcript expression in somatic tissue, particularly in a tissue in which we know its function is critical. This revealed a significant relationship between gene expression in *Nxt1* mutants and intron length for

both down and up regulated genes. For down-regulated genes, the more dramatic the down-regulation, the longer the total intron length. Similarly, for up regulated genes, the more up regulated the gene, the shorter the total intron length. The RNA seq data of both whole larvae and larval carcasses revealed no strong changes in EJC component transcripts. Therefore it is unlikely that defects in EJC component expression levels are implicated in the phenotype. However clearly the ratio between EJC, Nxf1 and Nxt1 will be affected when the level of active Nxt1 is reduced. During primary transcript processing, the spliceosome removes the intron and then the EJC is recruited to the mRNA [35]. The EJC recruits the THO complex, which also recruits UAP56 and REF to form the TREX complex [43]. UAP56 is displaced by the Nxt1-Nxf1 dimer, binding to REF, then REF is removed from the mRNP and Nxt1-Nxf1 binds directly to the mRNP [44]. This process occurs at every intron, and therefore, transcripts with many introns have more Nxt1-Nxf1 dimer recruitment. If EJC loading is less efficient on transcripts with long introns, then these transcripts could be preferentially sensitive to the Nxt1 trans-heterozygotes where the availability of Nxt1 protein is limiting.

Circular RNAs are a relatively recently described class of RNAs that are produced as alternative products from the same primary transcripts as mRNAs. Global analysis of circRNA abundance reveals that many genes can encode circRNAs, but the propensity for a gene to produce a circular transcript is related to the length of the introns, particularly those that flank the back-spliced exon(s) [10]. Our RNAseq analysis suggests that the mRNAs from genes that also produce circRNAs is reduced in Nxt1 mutants. Mutation of exon junction complex components has also been shown to have a preferential effect on mRNA production from genes with long introns [36]. At least some genes down-regulated in the EJC knock down have been shown to have aberrant splicing patterns in the absence of EJC [36]. In contrast, we found few defects in alternative splicing in *Nxt1* mutants. However, it is also interesting to note that 249/315 genes down-regulated after knock down of the EJC were also on the list of genes that produce at least one circRNA, and 99 are on the higher confidence list of 10 or more circRNAs [13, 36]. In light of this, it is likely that the EJC and the export adapter Nxt1 (and presumably Nxf1) are particularly important in processing of transcripts that could be destined to produce circular RNA outputs. This would involve either the EJC and export factors directly interacting with the splicing regulators, or a feedback mechanism, where later aspects of RNA processing affect the upstream activities. It will be very interesting to determine the global effect on circRNA levels themselves in conditions where Nxt1 or the EJC are limiting.

RNA regulation, and particularly RNA splicing has been linked to muscular degenerative diseases [18]. It is believed that sequestration of the splicing regulator MBNL1 by RNA containing expanded CUG or CCUG repeats reduces functional MBNL and results in aberant splicing of downstream targets in DM patients. The *Drosophila* orthologue of MBNL1, *mbl*, produces an abundant circRNA

similarly one of the many MBNL1 splice variants in humans is a circRNA [11]. *mbl* is expressed in both muscles and the nervous system, and is one of the many circRNA-producing genes whose mRNA is reduced (approximately 10x) in *Nxt1* mutant larvae. The production of the *mbl* circRNA is regulated by Mbl protein itself, in an autoregulatory feedback loop. In vertebrates it appears that MBNL1 does not regulate production of its own circRNA in neuronal cells, but the effect in muscle has not been determined [19, 45]. Our discovery that defects in an RNA export factor, Nxt1, can generate a muscular dystrophy phenotype in *Drosophila* suggest that investigation of the RNA export pathway in context of the disease is warranted.

Materials and Methods

Drosophila culture, strains and genetics.

Flies were maintained in standard cornmeal, yeast, dextrose, agar medium, at 25°C unless otherwise stated. For selection of staged larvae, 0.05% bromophenol blue was added to the food. Wandering larvae have blue guts, whereas stationary larvae have no blue or very light blue guts. White prepupae were selected by watching larvae, and harvesting them within an hour of pupariation. w^{1118} was used as a control. *yw ; Nxt1*$^{z2\text{-}0488}$ */ CyO Actin-GFP* and *yw ; Nxt1* ^{DG05102} */ CyO Actin-GFP* were crossed to generate *Nxt1*$^{z2\text{-}0488}$ */ Nxt1* ^{DG05102} transheterozygotes for analyses [20]. The *Nxt1* mutant larvae were selected by the absence of GFP.

Two VDRC Nxt1 RNAi lines, P{KK107745}VIE-260B (Nxt1 RNAi 103146) and w^{1118};P{GD17336}v52631 (Nxt1 RNAi 52631), were used to analyse muscle integrity in the third instar larvae [21]. 103146 has a 286bp hairpin length with predictions of 1 ON and 1 OFF targets, whereas 52631 has a 340bp length with 1 ON and 0 OFF targets predicted. UAS-eGFP-Nxt1 was described in [20].

w;UAS-*abba*^{fl}, kindly provided by Hanh T. Nguyen, uses the EST GH06739 (GenBank accession number AY121620) as template to amplify and clone the entire *abba* coding or defined regions of *abba* into the pUAST vector [22]. The 3' end of the construct encodes an HA tag. UAS-stock is in heterozygous condition. Mef2-Gal4 [23] was kindly provided by Michael Taylor (Cardiff University); Arm-Gal4 and UAS-dicer were from Bloomington stock centre.

RNA extraction, cDNA synthesis and Quantitative PCR

Total RNA was extracted using Trizol (ThermoFisher Scientific) and then further cleaned up with the RNeasy Mini Kit (Qiagen) according to manufacturer's protocol. The DNaseI step was included. RNA was quantified with a nanodrop ND-1000 (ThermoFisher Scientific) and stored at -80^{o}C. For larval carcass RNA sequencing, 30 carcasses were used per replicate in triplicates. For qRT-PCR, either a single carcass or a mix of up to 10 carcasses were used as detailed in the results. cDNA was

generated using 100ng total RNA and oligo dT primers with the Superscript III kit (Invitrogen). The cDNA reaction was diluted to 60 or 120µl with dH_2O, and 1µl of this cDNA was further diluted with 7µl dH_2O to use as a template in the qRT-PCR reactions. 10µl PowerSybr reagent (ABI) with 1µl of a 10µM solution of each target-specific forward and reverse primers (primer sequences on request) were added for a total reaction of 20µl. The qRT-PCR was performed on a Chromo4 instrument (MJR) using the Opticon Monitor 3 software. *Rp49* was used as a control gene for normalization, fold changes were determined by ΔΔCT. All reactions were performed in triplicate.

Scanning Electron Microscopy

Young pupae (<4h) were picked, cleaned with water, and air dried overnight. Up to 6 pupae were put on an aluminium backing plate of a SC500 sputter target. A BIO-RAD SC500 sputter coater was used to coat the non-conducting pupae with ~20nm thick layer of Au90Pd10 according to manufacturer's protocol (Quorum Technologies). After coating, pins were put in a FEI-XL30 Field Emission Gun Environmental Scanning Electron Microscope. For imaging, a 30 µm diameter final aperture with a beam current <1nA was used to take pictures from each pupa at the posterior/anterior end and the middle section.

Magnetic Chamber Dissection for larval muscle staining

For larval dissections, a magnetic chamber was used [24]. A magnetic strip, with a 30 mm diameter hole in the middle, was glued on a 76 mm x 51 mm slide with 10 mm of the strip sticking out at all sides. Each magnetic chamber uses 2 center and 4 corner pins. For constructing all pins, see figure 1 in [24]. All pins were glued to a vintage metal index tab. A larva is put in the middle of the hole with a drop of low Ca^{2+} saline, HL-3 [25]. Larva are put ventral side and two center pins are used to prevent the larva from moving by pinning at the most anterior and posterior side. Vannas Spring Scissors – 3mm blades (RS-5618; FineScience) were used for cutting. A dorsal incision cut was made at the posterior end with short shallow cuts between the two trachea until the anterior end was reached.

Phalloidin staining of larval muscles

The larva was cleaned on the magnetic chamber by removing all internal organs carefully. All Ca^{2+} saline, HL-3 solution was removed with a P-100 pipette and fresh drops were added two more times while cleaning the larval carcass. The larval carcass was fixated by adding fresh 4% paraformaldehyde in PBS for 2 minutes. All the pins were removed from the larval carcass and the sample was transferred to a glass well with 100µl 4% paraformaldehyde for another hour. The fixative was removed, and the larval carcass was washed twice with 100µl PBS-T (0.1% Triton X-100) for 5 minutes each. Two drops of Alexa Fluor™ 488 Phalloidin (ThermoFisher) was added to 1ml of PBS-T. 100µl Alexa Fluor™ 488 Phalloidin mix was added to the well to stain F-actin in larval muscles for 1 hour. Phalloidin solution was removed and the larval carcass was washed with PBS-T two times for 5 minutes each. The larva carcass was put on a microscope slide and mounted in

85% glycerol + 2.5% n-propyl gallate. Images were made on an Olympus BX 50 (Olympus) microscope and Hamamatsu ORCA-05G digital camera. For a close-up of the larval muscle sarcomeres pattern, images were taken with a Leica DM6000B upright microscope with HC PL Fluotar 20x/0.50 and HCX PL APO 40x/1.25 oil objectives.

Criteria for scoring muscle defects in larvae

The integrity of larva muscles was calculated as a percentage from a total of 8 hemisegments. The hemisegments A2-A5 were in the abdominal area and were not damaged by any of the pins. Each hemisegment contained 30 different muscles, so a total of 240 muscles were inspected. The integrity of a muscle is compromised if the muscle is damaged in any way, such as being torn, thin, loss of sarcomeric structure or missing. The muscle damage percentage is the total number of damaged muscles divided by 240 and multiplied by 100.

Starvation of larvae

Larvae were fed up to 70, 71, 72 and 73 hours after egg laying (AEL) before removal from the food. The larvae were transferred to a petri dish with a moist filter paper in it to prevent dessication. Larvae in the petri dish were checked at regular intervals to ensure the filter paper was moist and keep track of the progress of the metamorphosis. Larvae deprived of food 70 hours AEL that survived for four days were analysed for muscle integrity.

Mobility Assay

First, second and third instar larvae were used for mobility analysis. Larvae (up to 10) were put in the middle of a 1% agar dish with 1% paraffin oil on one side and an odor (1% 2-propanol) on the other side. Larvae were filmed with a Samsung SDN-550 camera using the micro manager 1.4 program for 200 frames, with 1 frame per second (fps) in the dark under red light. Movies were analysed with MtrackJ [26] via Fiji. Larvae were tracked per 20 frames (1^{st} instar) or 10 frames (2^{nd} and 3^{rd} instars) for at least 100 seconds (1^{st} instar) or 50 seconds (2^{nd} and 3^{rd} instar) while larvae were continuously crawling on the plate. Mean speed is calculated in mm/sec.

Viability Assay

Third instar larvae were taken from the standard vial and put in a new vial with a low quantity of fresh food for the viability assay. After 5 days of incubation at 25°C vials were taken out and pupa lethality was backtracked by looking at 6 different points: 1) larvae that did not pupate (0h APF), 2) no visible development in pupae (24h APF), 3) head eversion and development of the eye (48h APF), 4) bristles on dorsal thorax (72h APF), 5) complete fly development in pupa (72h APF) and 6) emerging adults.

RNA sequencing and analysis

Eighteen libraries were prepared from total RNA of w^{1118} and Nxt1 trans-heterozygotes genotypes. Each genotype had samples of three different stages (wandering larvae, stationary larvae and white

prepupae) in triplicates. RNA extraction was performed using Trizol (ThermoFisher Scientific) followed by the RNeasy Mini Kit (Qiagen). The samples were sent to the University of Exeter to perform the library preparation (ScriptSeq RNA-Seq Library Preparation Kit (Illumina)) and sequencing. All samples were 100bp paired-end sequenced on an Illumina HiSeq 2500 using standard mode.

Each sample was prepared in triplicates, and a sequence depth between 6.4M – 11.1M was achieved with sequencing all libraries. The data was analysed with the Tuxedo suite [27] via GenePattern browser [28]. The lists of genes and their Fragments per Kilobase of Exon per Million Mapped Fragments (FPKM) values were compared and statistically tested between the genotypes with Cuffdiff and were imported to excel and divided into more than 2-fold down regulated, more than 2-fold up regulated and non-differentially expressed lists. The differentially expressed genes were assigned statistically significant and had a p-value of <0.05.

Larval carcass RNAseq analysis

Six libraries were prepared from total RNA of w^{1118} and Nxt1 trans-heterozygotes genotypes. Stationary larvae from each genotype were taken and samples were generated in triplicates. RNA extraction was performed using a combination of Trizol (ThermoFisher Scientific) and the RNeasy Mini Kit (Qiagen). Libraries were generated using the TruSeq Stranded mRNA Library Prep (Illumina) according to manufacturer's protocol. Samples were sequenced using 2x75bp paired-end with the NextSeq 500/550 Mid Output v2 kit (150 cycles; Cat. No. FC-404-2001) on an Illumina NextSeq500 Sequencer (Illumina).

Each library achieved a read depth between 21M to 32M reads and the data was analysed through the Tuxedo suite [27]. The list of genes with FPKM values provided by Cuffdiff was used to separate the lists in more than 1.5-, 2-, 4- and 16-fold down regulated, more than 1.5-, 2-, 4- and 16-fold up regulated and non-differentially expressed. The differentially expressed genes that were assigned statistically significant had a p-value of <0.05. For graphical display on log axes, 0.001 was added to all FPKM values.

Acknowledgments

We gratefully acknowledge all members of the Cardiff University Drosophila community, and particularly Sonia Lopez de Quinto, Michael Taylor and Wynand van der Goes van Naters for helpful input on experimental design and data interpretation throughout the project. Drosophila stocks were provided by Michael Taylor (Cardiff), Hanh T. Nguyen (), Vienna Drosophila Resource Centre and

615 Bloomington Drosophila Stock Centre. RNAseq was carried out by Exeter University sequencing
616 service.

617

618 **Data availability**

619 RNAseq datasets for whole larvae (*w1118* and *Nxt1* transheterozygotes) before, during and after
620 puparium formation, and late third instar larval carcass samples are available via GEO, accession
621 numbers GSE125781 and GSE125776 respectively.

622

623

624

625 **Figure Legends**

626 **Figure 1 Morphological defects in Nxt1 trans-heterozygote pupae.** A) Nxt1 mutant pupae are
627 typically thinner than wild type, are curved, and have uneverted spiracles. B) Axial ratios show Nxt1
628 mutants are thinner and longer than wild type. C-E) Scanning electron microscopy shows details of
629 anterior and posterior spiracles wild type and Nxt1 mutant pupal cases. Figure in A was taken from
630 [20].

631

632

633 **Figure 2**

634 **Air bubble movement fails in Nxt1 trans-heterozygote pupae.** Still images of wild type (upper)
635 and Nxt1 trans-heterozygotes (lower) for 15 hours. A) Faint visibility of air bubble in both genotypes.
636 B-D) Air bubble becomes more prominent. E-G) Air bubble is clearly visible halfway along the pupa.
637 I-L) Air bubble expands further. M) Air bubble has disappeared and permitted head eversion for wild
638 type, whereas Nxt1 mutant still show air bubble. N) Larva body in Nxt1 mutant released from cuticle
639 at posterior end and retracts to anterior. O-P) No further changes observed in both genotypes.

640

641

642

643 **Figure 3**

644 **Nxt1 trans-heterozygote 3rd instar larvae have reduced mobility.** A-B) Image of agar plate and
645 larval tracks (analysed via MtrackJ) with control substance on the left and odor on the right. C-E)
646 Mobility analysis of 1st, 2nd and 3rd instars of wild type and Nxt1 trans-heterozygotes. F-G) All 1st, 2nd

and 3rd instar data combined for each genotype. Student's t-test *** p value = <0.001. n.s = not significant.

Figure 4

Nxt1 trans-heterozygote 3rd instar larvae show muscle degeneration. Muscles of larval carcass preparations (WT A and C, Nxt1 mutants B and D-K) imaged with FITC-phalloidin. A) Overview of wild type 3rd instar larva muscles. B) Overview of $Nxt1^{DG05102}/Nxt1^{Z2-0488}$ 3rd instar larva muscles. C) Higher power image of larva hemisegments from (A). D) Hemisegments from $Nxt1^{DG05102}/Nxt1^{Z2-0488}$ with mild muscle degeneration. E) Higher power image of larva hemisegments from (B). F) Lateral Transverse (LT) 1 and 2 crossover (short arrow). F-G) Short LT4 muscle (long arrow). H) Lateral Oblique (LO) 1 fiber split (red arrow). I) J) LO 1 partially degenerated into small bundle of fibers connected to the Segment Border Muscle (SBM). K) Dorsal Oblique (DO) 2 showing strings of fibers (red dotted lines) attached to each end of the muscle. Samples orientated from posterior (left) to anterior (right). A-E) Scale bar = 1 mm. F-K) Scale bar = 200 µm.

Figure 5

Nxt1 trans-heterozygote muscles do not degenerate when larval growth is prevented. A) Nxt1 trans-heterozygote pupae were smaller, but had normal morphology when food was withheld from 70h AEL. Three food-deprived and three normal feeding animals are shown. B) Nxt1 trans-heterozygote 70h AEL were examined for muscle degeneration. Individuals that had not pupated four days after no feeding still had intact muscles (N= 10).

Figure 6

Increasing *abba* expression rescues Nxt1 trans-heterozygote muscle degeneration. A) Genomic structure of the longest *abba* transcript including all known domains, exons are broad boxes, introns are narrow lines. B) Q-RT-PCR analysis of expression of *abba* in 10 individual stationary larvae plus a mix of 30 stationary larvae in Nxt1 trans-heterozygotes, compared to a mix of 10 and 30 stationary wild type larvae, respectively. C) Increasing *abba* with the UAS/Gal4 system specifically in muscles rescues muscle degeneration, as revealed by FITC-phalloidin staining. D) Expression of *abba* in 10 individual larvae from the rescue experiment, compared to a mix of 10 stationary wild type larvae. Rp49 was used for normalization.

Figure 7

Reduced expression of spliced but not nascent *abba* transcripts in Nxt1 trans-heterozygotes. A) Overview of six different *abba* isoforms, including the four regions used for nascent vs. spliced transcript analysis. B) qRT-PCR of four different regions in *abba* comparing nascent vs. spliced expression. Rp49 was used for normalization.

Figure 8. Genes with long introns are under-expressed in Nxt1 trans-heterozygotes.

mRNA level (FPKM) showing relative expression in WT and Nxt1 larval carcass samples. A) All genes, coloured to show total intron length. Genes with long introns are typically expressed at lower levels in the mutant than in the wild type sample. B) Genes (red in panel A) whose total intron length is >50kb, C) Genes (yellow in panel A) whose total intron length is between 15 and 50 kb, D) Genes (green in panel A) whose total intron length is between 5 and 15kb, E) Genes (blue in panel A) whose total intron length is <5 kb, F) Genes (black in panel A) without introns.

Figure 9

Q-RT-PCR validation of under-expression of genes with long introns in Nxt1 trans-heterozygote larval carcass. Genes with an average total intron length of 5700, 7500, 10000 and 15000 were examined. Expression of Abba and Nxt1 are also shown. CG1307 and CG9330 were used as control genes with low total intron length. All genes examined have expression in the carcass. Rp49 was used for normalization.

Table 1

Total intron lengths for genes down and up regulated from larval skin sequencing. Genes down regulated have longer total intron length compared to up regulated and non-differentially expressed genes. The total intron length becomes longer with the more highly down regulated genes. Down regulated genes have more introns and their largest intron is significantly longer.

Table 2

Transcript lengths from down and up regulated genes. Genes that are down regulated also have a longer transcript length compared to up regulated and non-differentially expressed genes. For down regulated genes, the number of transcripts is higher and their shortest/longest transcripts are larger.

Figure S1

Sarcomere structure compromised in degenerating muscles. A) Wild type muscles stained for actin with phalloidin show normal, ribbed lines, thin filaments. B) Nxt1 trans-heterozygotes non-degenerating muscles with normal, ribbed lines, thin filaments. C) Nxt1 trans-heterozygotes degenerating muscles with compromised thin filaments.

Figure S2

Early 2nd instar muscle degeneration with Nxt1 RNAi. A-A') Wild type 2nd instar larvae carcass preparations, stained with phalloidin, showing normal muscle composition and no damage. B-B') Signs of muscle degeneration with the RNAi 103146 line driven by Mef2-Gal4 visible in early 2nd instars with thinner muscles and fiber damage (see insert B'). C-C') Similar degeneration defects shown for the RNAi 52631 line. A-C) Scale bar = 1mm. A'-C') Scale bar = 0.5mm.

Figure S3

Timing of pupal lethality in Nxt1 trans-heterozygotes. Pupae were examined at six different time points. Many Nxt1 mutants had defects in head eversion, which becomes visible 48 hours into the pupa phase. Nxt1 hypomorph/+ heterozygotes showed a slight reduction in pupa viability.

Figure S4

Rescue of Nxt1 trans-heterozygote phenotypes. Nxt1 transheterozygote defects in viability (A), pupal morphology (axial ratios of pupae, B), muscle morphology (C) and 3rd instar motility (D) were partially rescued by over-expression of GFP-Nxt1 in muscles (Mef2-Gal4) or ubiquitously (arm-Gal4).

Supp table 1

Known ecdysone responsive genes are not under-expressed in Nxt1 trans-heterozygotes. Ecdysone responsive genes [30] were examined by looking their differential expression status in whole larval RNAseq data from cuffdiff (P-value <0.05), a minimum fold change of 2 and a FPKM threshold of at least 10 FPKM in one of the two genotypes.

Supp table 2

Overview of larval muscle genes from whole larval RNA sequencing. Thirteen larval muscle genes with log2 fold change from RNA sequencing showing majority of genes up regulated with only

one down regulated. Red = more than 1.5-fold down regulated. Green = more than 1.5-fold up regulated

References

1. Bate M. The embryonic development of larval muscles in Drosophila. Development (Cambridge, England). 1990;110(3):791-804.
2. Kim JH, Jin P, Duan R, Chen EH. Mechanisms of myoblast fusion during muscle development. Current opinion in genetics & development. 2015;32:162-70. Epub 2015/05/20. doi: 10.1016/j.gde.2015.03.006. PubMed PMID: 25989064; PubMed Central PMCID: PMCPMC4508005.
3. Piccirillo R, Demontis F, Perrimon N, Goldberg AL. Mechanisms of muscle growth and atrophy in mammals and Drosophila. Developmental Dynamics. 2014;243(2):201-15. doi: 10.1002/dvdy.24036.
4. Shatoury HH. The Development of a Pupal Lethal Mutant in Drosophila. Caryologia. 1959;12:1:104-9.
5. Carmody SR, Wente SR. mRNA nuclear export at a glance. J Cell Sci. 2009;122:1933-7.
6. Strasser K, Masuda S, Mason P, Pfannstiel J, Oppizzi M, Rodriguez-Navarro S, et al. TREX is a conserved complex coupling transcription with messenger RNA export. Nature. 2002;417(6886):304-8. Epub 2002/04/30. doi: 10.1038/nature746. PubMed PMID: 11979277.
7. Boehm V, Gehring NH. Exon Junction Complexes: Supervising the Gene Expression Assembly Line. Trends in Genetics. 2016;32(11):724-35. doi: https://doi.org/10.1016/j.tig.2016.09.003.
8. Huang S, Yang B, Chen BJ, Bliim N, Ueberham U, Arendt T, et al. The emerging role of circular RNAs in transcriptome regulation. Genomics. 2017;109(5):401-7. doi: https://doi.org/10.1016/j.ygeno.2017.06.005.
9. Li X, Yang L, Chen L-L. The Biogenesis, Functions, and Challenges of Circular RNAs. Molecular Cell. 2018;71(3):428-42. doi: https://doi.org/10.1016/j.molcel.2018.06.034.
10. Jeck WR, Sorrentino JA, Wang K, Slevin MK, Burd CE, Liu J, et al. Circular RNAs are abundant, conserved, and associated with ALU repeats. RNA (New York, NY). 2013;19(2):141-57.
11. Ashwal-Fluss R, Meyer M, Pamudurti Nagarjuna R, Ivanov A, Bartok O, Hanan M, et al. circRNA Biogenesis Competes with Pre-mRNA Splicing. Molecular Cell. 2014;56(1):55-66. doi: https://doi.org/10.1016/j.molcel.2014.08.019.
12. Zhang Y, Xue W, Li X, Zhang J, Chen S, Zhang J-L, et al. The Biogenesis of Nascent Circular RNAs. Cell Reports. 2016;15(3):611-24. doi: https://doi.org/10.1016/j.celrep.2016.03.058.
13. Westholm Jakub O, Miura P, Olson S, Shenker S, Joseph B, Sanfilippo P, et al. Genome-wide Analysis of Drosophila Circular RNAs Reveals Their Structural and Sequence Properties and Age-Dependent Neural Accumulation. Cell Reports. 2014;9(5):1966-80. doi: https://doi.org/10.1016/j.celrep.2014.10.062.

14. Hoffman EP, Brown RH, Kunkel LM. Dystrophin: The protein product of the duchenne muscular dystrophy locus. Cell. 1987;51(6):919-28. doi: https://doi.org/10.1016/0092-8674(87)90579-4.
15. Peter AK, Cheng H, Ross RS, Knowlton KU, Chen J. The costamere bridges sarcomeres to the sarcolemma in striated muscle. Progress in pediatric cardiology. 2011;31(2):83-8. doi: 10.1016/j.ppedcard.2011.02.003. PubMed PMID: 24039381.
16. Frosk P, Weiler T, Nylen E, Sudha T, Greenberg CR, Morgan K, et al. Limb-girdle muscular dystrophy type 2H associated with mutation in TRIM32, a putative E3-ubiquitin-ligase gene. American journal of human genetics. 2002;70(3):663-72. Epub 01/29. doi: 10.1086/339083. PubMed PMID: 11822024.
17. Meola G, Cardani R. Myotonic dystrophies: An update on clinical aspects, genetic, pathology, and molecular pathomechanisms. Biochimica et Biophysica Acta (BBA) - Molecular Basis of Disease. 2015;1852(4):594-606. doi: https://doi.org/10.1016/j.bbadis.2014.05.019.
18. Wheeler TM, Thornton CA. Myotonic dystrophy: RNA-mediated muscle disease. Current Opinion in Neurology. 2007;20(5):572-6. doi: 10.1097/WCO.0b013e3282ef6064. PubMed PMID: 00019052-200710000-00011.
19. Konieczny P, Stepniak-Konieczna E, Sobczak K. MBNL expression in autoregulatory feedback loops. RNA Biology. 2018;15(1):1-8. doi: 10.1080/15476286.2017.1384119.
20. Caporilli S, Yu Y, Jiang J, White-Cooper H. The RNA export factor, Nxt1, is required for tissue specific transcriptional regulation. PLoS genetics. 2013;9(6):e1003526. Epub 2013/06/12. doi: 10.1371/journal.pgen.1003526. PubMed PMID: 23754955; PubMed Central PMCID: PMCPmc3674997.
21. Dietzl G, Chen D, Schnorrer F, Su K, Barinova Y, Fellner M, et al. A genome-wide transgenic RNAi library for conditional gene inactivation in Drosophila. Nature. 2007;448:151-6.
22. Domsch K, Ezzeddine N, Nguyen HT. Abba is an essential TRIM/RBCC protein to maintain the integrity of sarcomeric cytoarchitecture. J Cell Sci. 2013;126(Pt 15):3314-23. Epub 2013/06/05. doi: 10.1242/jcs.122366. PubMed PMID: 23729735.
23. Ranganayakulu G, Schulz RA, Olson EN. Wingless Signaling InducesnautilusExpression in the Ventral Mesoderm of theDrosophilaEmbryo. Developmental Biology. 1996;176(1):143-8. doi: https://doi.org/10.1006/dbio.1996.9987.
24. Budnik V, Gorczyca M, Prokop A. Selected methods for the anatomical study of drosophila embryonic and larval neuromuscular junctions. Budnik V, Ruiz-Canada C, editors: International Review of Neurobiology; 2006.
25. Pesavento PA, Stewart RJ, Goldstein LSB. Characterization of the KLP68D kinesin-like protein in *Drosophila*: possible roles in axonal transport. J Cell Biol. 1994;127(4):1041-8.
26. Meijering E, Dzyubachyk O, Smal I. Methods for cell and particle tracking. Methods in enzymology. 2012;504:183-200. Epub 2012/01/24. doi: 10.1016/b978-0-12-391857-4.00009-4. PubMed PMID: 22264535.
27. Trapnell C, Roberts A, Goff L, Pertea G, Kim D, Kelley DR, et al. Differential gene and transcript expression analysis of RNA-seq experiments with TopHat and Cufflinks. Nat Protoc. 2012;7(3):562-78. Epub 2012/03/03. doi: 10.1038/nprot.2012.016. PubMed PMID: 22383036; PubMed Central PMCID: PMCPMC3334321.
28. Reich M, Liefeld T, Gould J, Lerner J, Tamayo P, Mesirov JP. GenePattern 2.0. Nature genetics. 2006;38(5):500-1. Epub 2006/04/28. doi: 10.1038/ng0506-500. PubMed PMID: 16642009.
29. Yamanaka N, Rewitz KF, O'Connor MB. Ecdysone control of developmental transitions: lessons from Drosophila research. Annual review of entomology. 2013;58:497-516. Epub 10/15. doi: 10.1146/annurev-ento-120811-153608. PubMed PMID: 23072462.
30. Fletcher JC, Thummel CS. The Drosophila E74 gene is required for the proper stage- and tissue-specific transcription of ecdysone-regulated genes at the onset of metamorphosis. Development (Cambridge, England). 1995;121(5):1411-21. Epub 1995/05/01. PubMed PMID: 7789271.
31. Wright LG, Chen T, Thummel CS, Guild GM. Molecular characterization of the 71E late puff in Drosophila melanogaster reveals a family of novel genes. J Mol Biol. 1996;255(3):387-400. Epub 1996/01/26. doi: 10.1006/jmbi.1996.0032. PubMed PMID: 8568884.
32. Vaskova M, Bentley AM, Marshall S, Reid P, Thummel CS, Andres AJ. Genetic analysis of the Drosophila 63F early puff. Characterization of mutations in E63-1 and maggie, a putative Tom22.

847 Genetics. 2000;156(1):229-44. Epub 2000/09/09. PubMed PMID: 10978288; PubMed Central
848 PMCID: PMCPMC1461229.
849 33. Beadle GW, Tatum EL, Clancy CW. Food level in relation to rate of development and eye
850 pigmentation in Drosophilha melanogaster. Bio Bull. 1938;75(3):447-62.
851 34. LaBeau-DiMenna EM, Clark KA, Bauman KD, Parker DS, Cripps RM, Geisbrecht ER. Thin,
852 a Trim32 ortholog, is essential for myofibril stability and is required for the integrity of the costamere
853 in Drosophila. Proceedings of the National Academy of Sciences of the United States of America.
854 2012;109(44):17983-8. Epub 10/15. doi: 10.1073/pnas.1208408109. PubMed PMID: 23071324.
855 35. Le Hir H, Gatfield D, Izaurralde E, Moore M. The exon-exon junction complex provides a
856 binding platform for factors involved in mRNA export and nonsense-mediated mRNA decay. EMBO
857 J. 2001;20:4987-97.
858 36. Ashton-Beaucage D, Udell CM, Lavoie H, Baril C, Lefrançois M, Chagnon P, et al. The Exon
859 Junction Complex Controls the Splicing of mapk and Other Long Intron-Containing Transcripts in
860 Drosophila. Cell. 2010;143(2):251-62. doi: https://doi.org/10.1016/j.cell.2010.09.014.
861 37. Duff MO, Olson S, Wei X, Garrett SC, Osman A, Bolisetty M, et al. Genome-wide
862 identification of zero nucleotide recursive splicing in Drosophila. Nature. 2015;521:376. doi:
863 10.1038/nature14475
864 https://www.nature.com/articles/nature14475 - supplementary-information.
865 38. Herold A, Klymenko T, Izaurralde E. NXF1/p15 heterodimers are essential for mRNA nuclear
866 export in Drosophila. RNA. 2001;7:1768-80.
867 39. Wiegand HL, Coburn GA, Zeng Y, Kang Y, Bogerd HP, Cullen BR. Formation of Tap/NXT1
868 heterodimers activates Tap-dependent nuclear mRNA export by enhancing recruitment to nuclear
869 pore complexes. Mol Cell Biol. 2002;22(1):245-56. Epub 2001/12/12. PubMed PMID: 11739738;
870 PubMed Central PMCID: PMCPMC134221.
871 40. Demontis F, Perrimon N. Integration of Insulin receptor/Foxo signaling and dMyc activity
872 during muscle growth regulates body size in Drosophila. Development (Cambridge, England).
873 2009;136(6):983-93. Epub 2009/02/13. doi: 10.1242/dev.027466. PubMed PMID: 19211682;
874 PubMed Central PMCID: PMCPMC2727562.
875 41. Kudryashova E, Kudryashov D, Kramerova I, Spencer MJ. Trim32 is a ubiquitin ligase
876 mutated in limb girdle muscular dystrophy type 2H that binds to skeletal muscle myosin and
877 ubiquitinates actin. J Mol Biol. 2005;354(2):413-24. Epub 2005/10/26. doi:
878 10.1016/j.jmb.2005.09.068. PubMed PMID: 16243356.
879 42. Ashton-Beaucage D, Therrien M. The exon junction complex: a splicing factor for long intron
880 containing transcripts? Fly. 2011;5(3):224-33. Epub 2011/04/12. PubMed PMID: 21478676.
881 43. Strässer K, Masuda S, Mason P, Pfannstiel J, Oppizzi M, Rodriguez-Navarro S, et al. TREX
882 is a conserved complex coupling transcription with messenger RNA export. Nature. 2002;417:304-
883 8.
884 44. Strasser K, Hurt E. Yra1p, a conserved nuclear RNA-binding protein, interacts directly with
885 Mex67p and is required for mRNA export. EMBO J. 2000;19(3):410-20. Epub 2000/03/18. doi:
886 10.1093/emboj/19.3.410. PubMed PMID: 10722314; PubMed Central PMCID: PMCPMC305578.
887 45. Konieczny P, Stepniak-Konieczna E, Taylor K, Sznajder ŁJ, Sobczak K. Autoregulation of
888 MBNL1 function by exon 1 exclusion from MBNL1 transcript. Nucleic Acids Research.
889 2017;45(4):1760-75. doi: 10.1093/nar/gkw1158.

890

891

Fig. 1

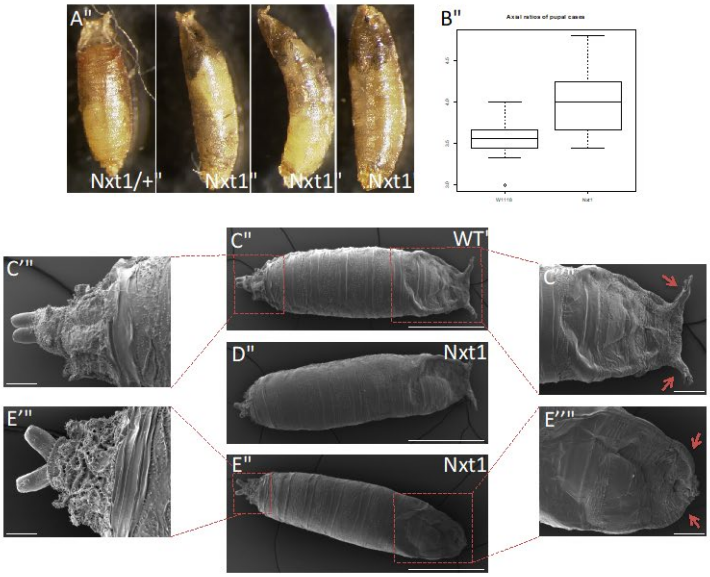

892

Fig. 2

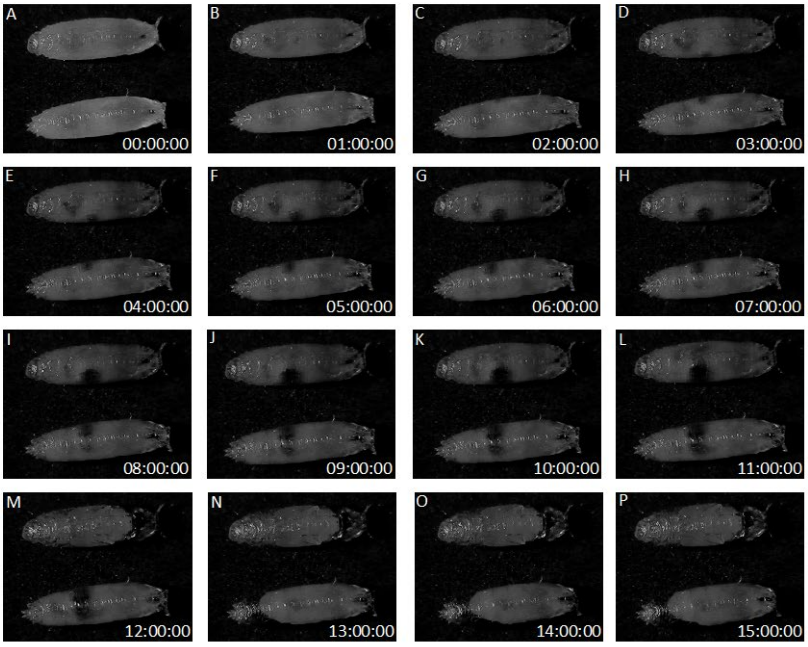

893

Fig. 3

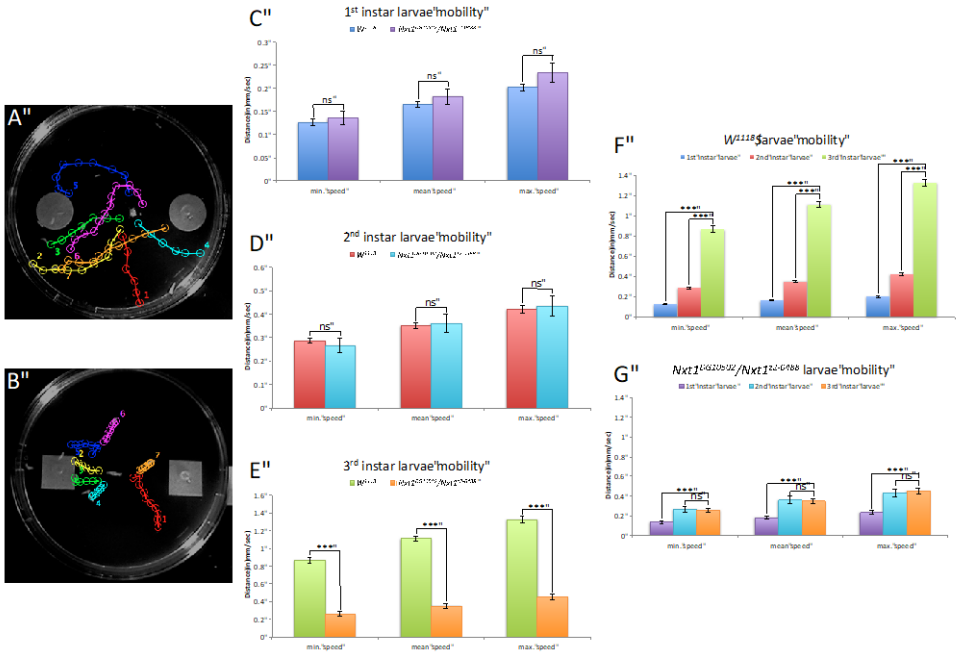

894

Fig. 4

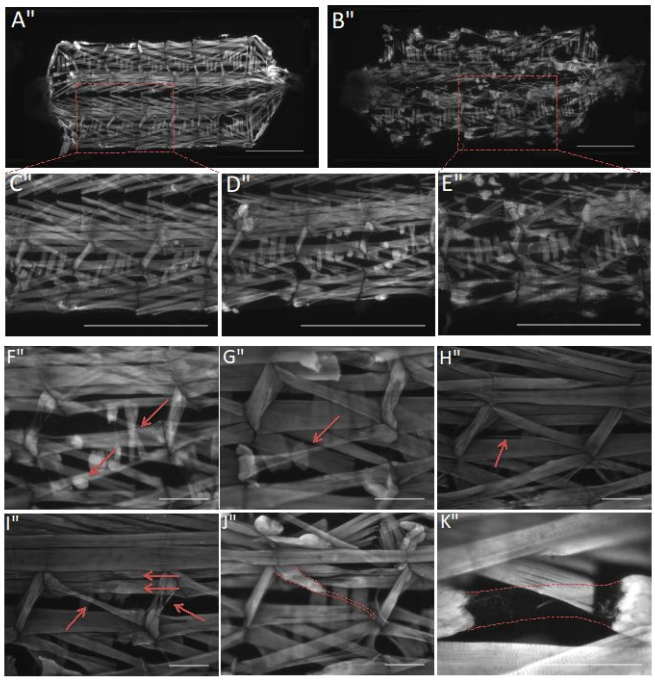

895

896

Fig. 5

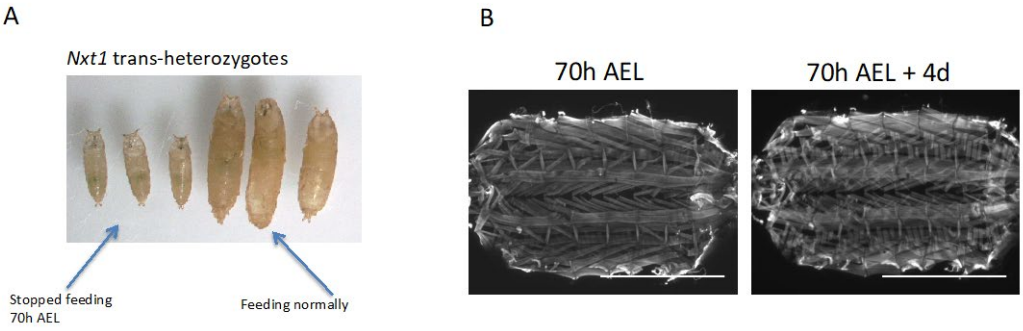

897

898

Fig. 6

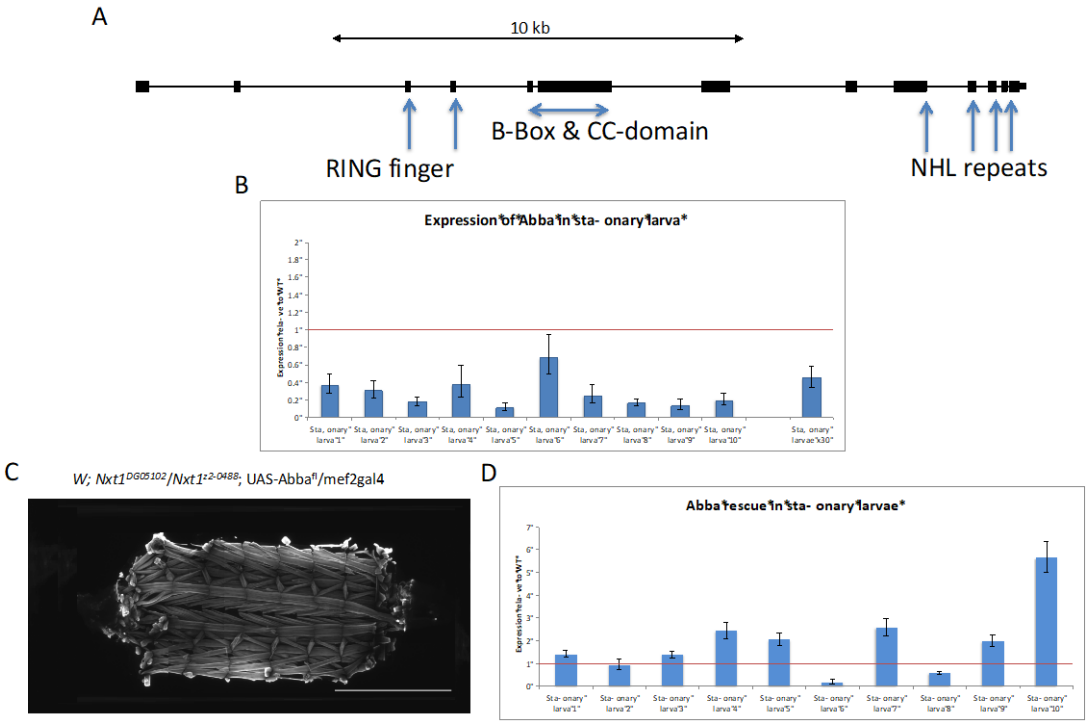

899

Fig. 7

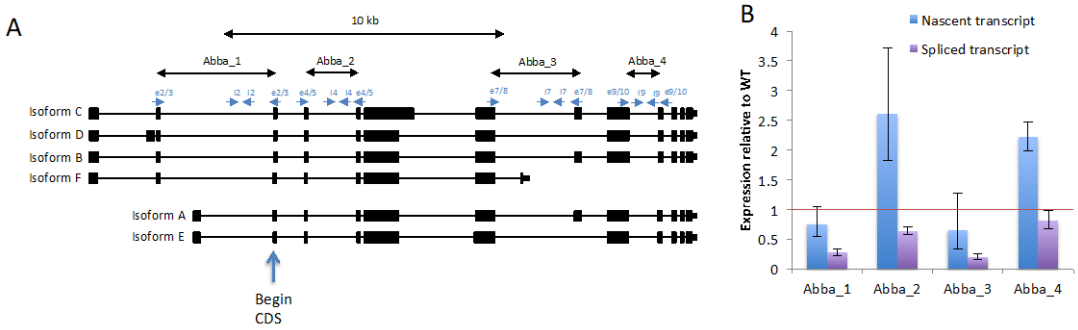

900

901

Fig. 8

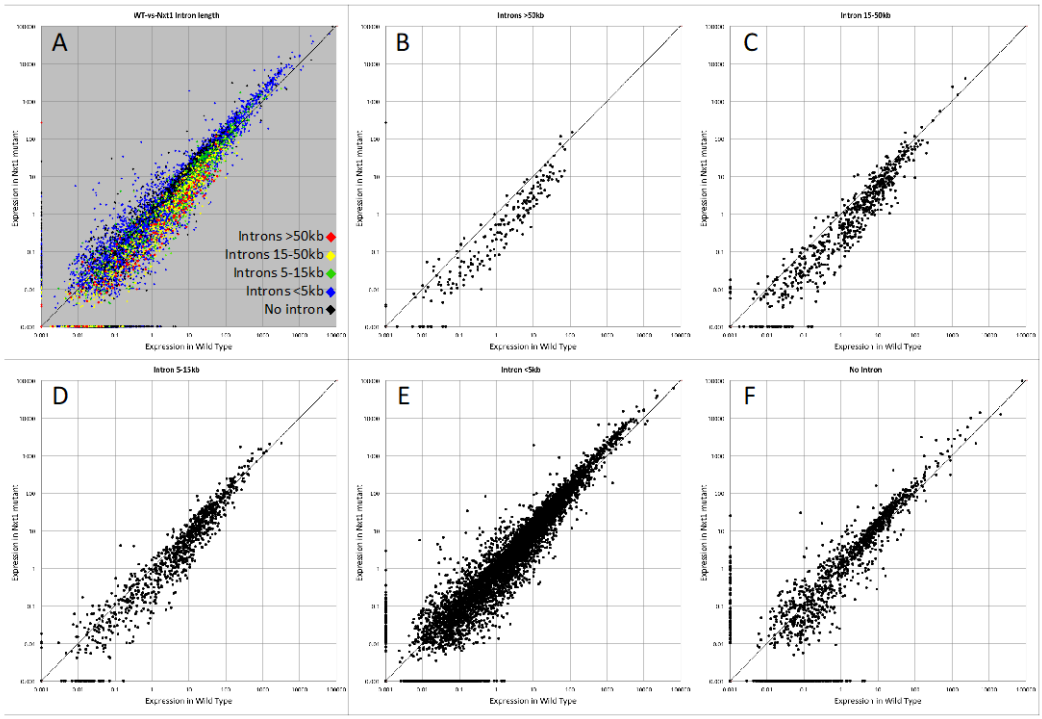

902

Fig. 9

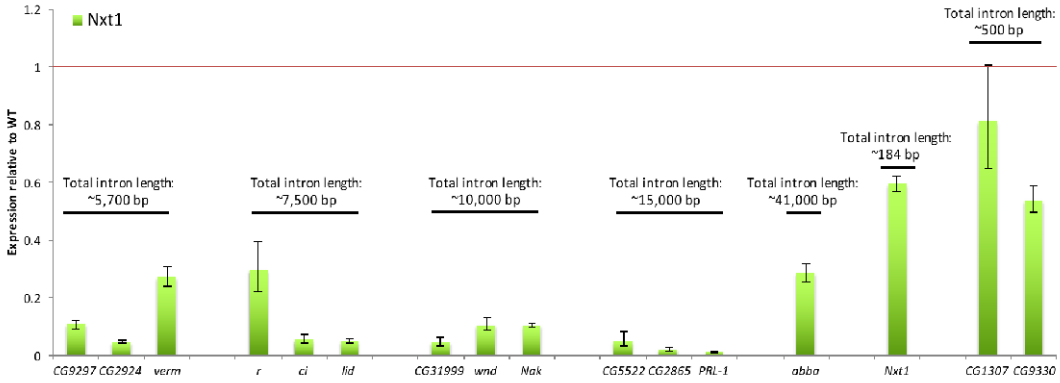

903

904

Table 1

Median	No. of genes	Total intron length	Number of introns	Smallest intron	Largest intron
Down-regulated >1.5 fold	1,821	5,769	9	59	2,341
Down-regulated >2 fold	1,340	7,594	9	59	2,931
Down-regulated >4 fold	567	10,201	11	59	3,642
Down-regulated >16 fold	32	15,254	10	63	8,081
Median	**No. of genes**	**Total intron length**	**Number of introns**	**Smallest intron**	**Largest intron**
Up-regulated >1.5 fold	1,339	368	3	62	160
Up-regulated >2 fold	572	352	3	62	155
Up-regulated >4 fold	89	237	2	62	133
Up-regulated >16 fold	15	238	2	61	180
Median	**No. of genes**	**Total intron length**	**Number of introns**	**Smallest intron**	**Largest intron**
Non-differentiated	4,754	497	4	60	228

905

Table 2

Median	No. of genes	Gene length	No. of transcripts	Shortest transcript	Longest transcript
Down-regulated >1.5 fold	1,821	8,440	3	3,220	4,263
Down-regulated >2 fold	1,340	9,706	3	3,301	4,533
Down-regulated >4 fold	567	12,162	3	3,722	5,168
Down-regulated >16 fold	32	14,213	4	3,486	5,761
Median	**No. of genes**	**Gene length**	**No. of transcripts**	**Shortest transcript**	**Longest transcript**
Up-regulated >1.5 fold	1,339	1,584	2	1.034	1,186
Up-regulated >2 fold	572	1,411	2	901	1,027
Up-regulated >4 fold	89	1,353	1	885	994
Up-regulated >16 fold	15	1,411	1	917	1,020
Median	**No. of genes**	**Gene length**	**No. of transcripts**	**Shortest transcript**	**Longest transcript**
Non-differentiated	4,754	2,496	2	1,642	1,856

908 Supplementary data

909

Sup. Table 1

Gene (wandering)	Differen7ally expressed?	Fold change (log2)	FPKM threshold?	Gene (sta7onary)	Differen7ally expressed?	Fold change (log2)	FPKM threshold?	Gene (prepupae)	Differen7ally expressed?	Fold change (log2)	FPKM threshold?
Br	NO	-0.10	YES	*Br*	NO	-0.20	YES	*Br*	NO	+0.02	YES
DHR3	NO	-0.31	NO	*DHR3*	NO	-0.87	YES	*DHR3*	NO	-0.35	YES
EcR	NO	-0.08	YES	*EcR*	NO	+0.44	YES	*EcR*	NO	+0.05	YES
Usp	NO	+0.54	YES	*Usp*	NO	+0.33	YES	*Usp*	NO	-0.14	YES
Ecd	NO	+0.28	YES	*Ecd*	NO	+0.24	YES	*Ecd*	NO	+0.36	YES
Edg78E	NO	+0.64	NO	*Edg78E*	NO	+2.15	NO	*Edg78E*	NO	+1.05	NO
Edg84A	NO	-	-	*Edg84A*	NO	-	-	*Edg84A*	NO	-	-
Edg91	NO	-0.05	YES	*Edg91*	NO	+0.46	YES	*Edg91*	NO	-0.16	NO
Eip55E	NO	+0.38	YES	*Eip55E*	NO	+0.30	YES	*Eip55E*	NO	0.00	YES
Eip63E	NO	0.00	YES	*Eip63E*	NO	-0.04	YES	*Eip63E*	NO	+0.36	YES
Eip63F-1	NO	-0.74	YES	*Eip63F-1*	YES	-0.97	YES	*Eip63F-1*	YES	+1.00	YES
Eip63F-2	NO	+0.26	NO	*Eip63F-2*	NO	+0.06	NO	*Eip63F-2*	NO	+0.85	NO
Eip71CD	YES	-0.87	YES	*Eip71CD*	NO	-0.47	YES	*Eip71CD*	NO	-0.18	YES
Eip74EF	NO	+0.03	YES	*Eip74EF*	NO	0.00	YES	*Eip74EF*	NO	+0.42	YES
Eip75B	NO	-0.37	YES	*Eip75B*	NO	-0.49	YES	*Eip75B*	NO	-0.30	YES
Eip78C	NO	-0.31	YES	*Eip78C*	NO	-0.37	YES	*Eip78C*	YES	+0.68	YES
Eip93F	NO	+0.35	NO	*Eip93F*	NO	-0.43	YES	*Eip93F*	NO	+0.29	YES
Ftz-f1	NO	+0.46	NO	*Ftz-f1*	NO	+0.66	NO	*Ftz-f1*	NO	-0.47	NO
Eig71Ea	NO	-1.18	YES	*Eig71Ea*	YES	-0.57	YES	*Eig71Ea*	NO	+0.32	YES
Eig71Eb	NO	-1.16	YES	*Eig71Eb*	YES	-1.62	YES	*Eig71Eb*	YES	-0.78	YES
Eig71Ec	NO	-2.16	NO	*Eig71Ec*	NO	-0.73	YES	*Eig71Ec*	NO	0.00	YES
Eig71Ed	NO	-1.27	YES	*Eig71Ed*	YES	-0.93	YES	*Eig71Ed*	YES	-0.42	YES
Eig71Ee	NO	-0.28	YES	*Eig71Ee*	NO	-0.08	YES	*Eig71Ee*	YES	+0.85	YES
Eig71Ef	NO	-2.44	NO	*Eig71Ef*	YES	-1.14	YES	*Eig71Ef*	NO	-0.34	YES
Eig71Eg	NO	-1.99	YES	*Eig71Eg*	YES	-1.55	YES	*Eig71Eg*	YES	-0.97	YES
Eig71Eh	NO	-	-	*Eig71Eh*	NO	-3.34	NO	*Eig71Eh*	YES	-1.48	YES
Eig71Ei	NO	-	-	*Eig71Ei*	NO	-2.50	NO	*Eig71Ei*	NO	-0.75	YES
Eig71Ej	NO	-	-	*Eig71Ej*	NO	-	-	*Eig71Ej*	NO	-0.92	NO
Eig71Ek	NO	-	-	*Eig71Ek*	NO	-	-	*Eig71Ek*	NO	+1.21	NO

910

911

Sup. Table 2

Gene name	Log2 fold change
abba	-0.75
up	+1.54
Arc1	+1.84
Prm	+1.62
Mlc2	+2.16
Mhc	+3.02
Act57B	+2.04
mib2	-0.48
Mlp84B	+0.88
Actn	+0.33
Mp20	+2.08
wupA	+0.90
sls	+0.16

Fig. S1

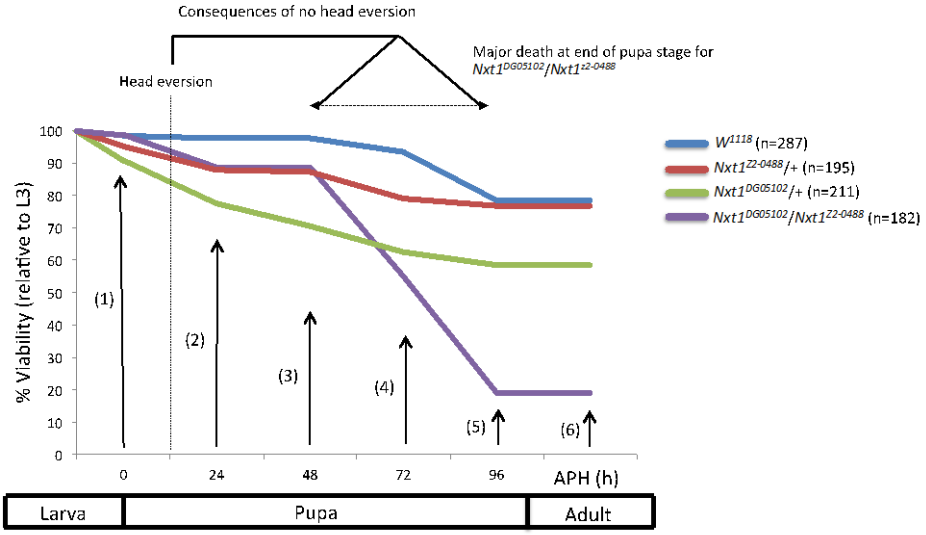

(1): Larvae that did not pupate
(2): No visible development in pupa
(3): Eye starts developing
(4): Bristles on thorax visible
(5): Complete fly development in pupa
(6): Adults that emerged

915

Sup. Fig. 2

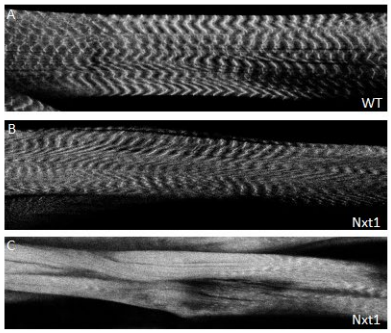

916

917

Sup. Fig. 3

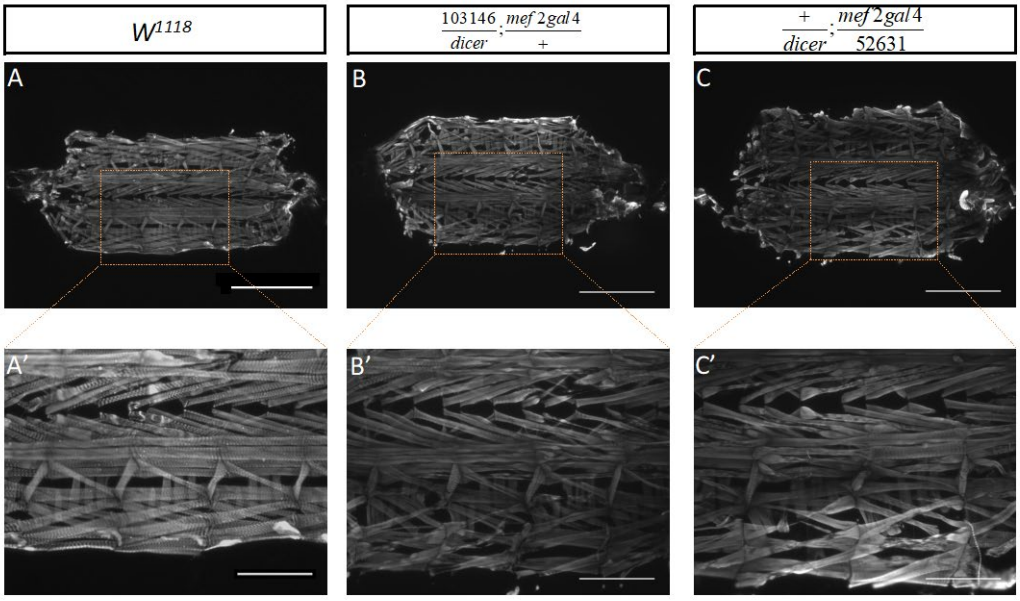

Sup. Fig. 4